Isothermal and Nonisothermal Cure Kinetics of an Epoxy/Poly(oxypropylene)diamine/Octadecylammonium Modified Montmorillonite System

Ivan Brnardic, Marica Ivankovic, Hrvoje Ivankovic, Helena Jasna Mencer

Faculty of Chemical Engineering and Technology, University of Zagreb, HR-10001 Zagreb, Marulicev trg 19, p.p. 177, Croatia

Received 20 October 2004; accepted 22 June 2005
DOI 10.1002/app.23080
Published online 23 January 2006 in Wiley InterScience (www.interscience.wiley.com).

ABSTRACT: The effect of an octadecylammonium-exchanged montmorillonite on the curing kinetics of a thermoset system based on a bisphenol A epoxy resin and a poly(oxypropylene)diamine curing agent were studied with differential scanning calorimetry (DSC) in isothermal and dynamic (constant-heating-rate) conditions. Montmorillonite and the prepared composites were characterized by X-ray diffraction analysis and simultaneous DSC and thermogravimetric analysis. The analysis of the DSC data indicated that the intercalated octadecylammonium cations catalyzed the epoxy–amine polymerization. A kinetic model, arising from an autocatalyzed reaction mechanism, was applied to the DSC data. Fairly good agreement between the experimental data and the modeling data was obtained. © 2006 Wiley Periodicals, Inc. J Appl Polym Sci 100: 1765–1771, 2006

Key words: differential scanning calorimetry (DSC); kinetics (polym.); nanocomposites

INTRODUCTION

The properties of polymer composites are greatly influenced by the length scale of their component phases. Nanoscale dispersion of inorganic fillers typically optimizes the mechanical properties of the composite. Layered silicates such as montmorillonite (MMT) have received considerable attention because of their potential in the preparation of polymer nanocomposites. Its rich intercalation chemistry allows it to be chemically modified and to become compatible with various polymers. Because of several influences, the morphology of the related nanocomposites can evolve from the so-called intercalated nanocomposites, where regular alternation of the layered silicates and polymer monolayers is observed, to the exfoliated (delaminated) type of nanocomposites, where individual nanometer-thick silicate layers are randomly and homogeneously distributed throughout the polymer matrix. Generally, exfoliated nanocomposites exhibit better properties than intercalated composites.

Epoxy resins are widely used as polymer matrices for composites. Research on layered silicate–epoxy nanocomposites has gained widespread attention in recent years.[1–17] In general, epoxy resin curing reactions involve the opening of the epoxide ring followed either by a homopolymerization reaction with further epoxide or a reaction with other species to form addition products. A great variety of poly(carboxylic acid anhydrides), aromatic diamines and aliphatic diamines, and polyamines are used as epoxy resin curing agents.

As is well known, the cure of epoxy resin involves the conversion of liquid monomers or prepolymers into crosslinking solids. The mechanism and kinetics of cure determine the network morphology and may influence the exfoliation behavior of layered silicates, which in turn, dictates the physical and mechanical properties of the cured product.

It has been shown previously[4] that MMTs intercalated by long-chain alkylammonium cations (with chain lengths larger than eight carbon atoms) favor clay-layer exfoliation and can catalyze the epoxy–amine polymerization reaction.

The curing kinetics of epoxy resins have been studied with different techniques, including Fourier transform infrared spectroscopy,[18,19] near-IR spectroscopy,[20] and differential scanning calorimetry (DSC).[21–26] However, the curing kinetics of epoxy resins during nanocomposite formation have been reported in few articles.[11,17]

In this study, the effect of octadecylammonium-exchanged montmorillonite (OMMT) on the curing kinetics of an epoxy resin based on diglycidyl ether of bisphenol A (DGEBA) was examined by means of DSC in both isothermal and dynamic modes. As a curing agent of the epoxy resin, a commercial poly(oxypropylene)diamine was used. A kinetic

Correspondence to: M. Ivankovic (mivank@fkit.hr).

TABLE I
Chemical Structure of the Materials Used

Epoxy—DGEBA

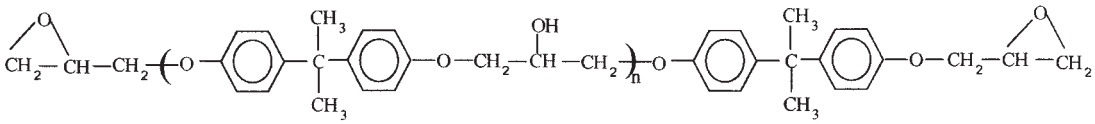

Poly(oxypropylene)diamine
$NH_2CHCH_3CH_2(OCH_2CHCH_3)_xNH_2$
D230 $x = 2.6$
Octadecylammonium
$CH_3—[CH_2]_{17}—NH_2$

model, arising from an autocatalyzed reaction mechanism, was applied to the DSC data. The MMT clay and prepared composites were characterized by X-ray diffraction (XRD) and simultaneous DSC and thermogravimetric analysis (TGA).

EXPERIMENTAL

Materials

The epoxy resin, DGEBA (DER 331), with an equivalent weight of 187 g/mol was obtained from Dow Chemicals (Midland, MI). Poly(oxypropylene) diamine, provided under the trade name Jeffamine D230 by Fluka (Buchs, Switzerland) and with a N—H equivalent weight of 57.5 g/mol, was used as a curing agent. The clay used was a Wyoming-type MMT provided by M. I. Drilling Fluids Co. (PorraQuay, Aberdeen, Scotland). Octadecylamine was provided by Kemika (Zagreb, Croatia). The materials were used as received. The chemical structures of the ingredients used are displayed in Table I.

Sample preparation and characterization

MMT clay was purified by means of standard sedimentation methods and converted to the Na^+ MMT form with a dilute NaCl aqueous solution. The cation exchange capacity was determined by the ammonium acetate method to be 101 mequiv/100 g. To prepare OMMT, a method described in the literature[8] was followed.

Before curing, the epoxy resin was mixed with the desired amount of OMMT (0, 5, and 10 g of OMMT per 100 g of epoxy) at 75°C for 24 h and sonicated for 15 min. After the mixture was cooled to room temperature, a stoichiometric amount of the curing agent Jeffamine D230 was added with thorough mixing for 60 min. The mixtures were poured into molds and cured at 80°C for 3 h followed by postcuring at 120°C for 1 h.

Part of the mixtures were characterized immediately by DSC. The calorimetric measurements were done on a Netzsch DSC 200 differential scanning calorimeter (Selb, Germany) operating in a nitrogen atmosphere. The sample size was around 15 mg. Dynamic DSC analysis was performed at three different heating rates: 3, 5, and 10°C/min. The sample was heated from room temperature to 250°C. We estimated the total heat of reaction (H_T) by drawing a straight line, connecting the base line before and after the peak, and integrating the area under the peak. Isothermal DSC experiments were performed at four temperatures. The reaction was considered complete when the curve leveled off to a baseline. After each isothermal run, the sample was cooled rapidly in the DSC cell to 30°C and then reheated at 10°C/min to 250°C to determine the residual heat of reaction (H_R). The digitized data were acquired by a computer and transferred to a PC for further treatment.

Dynamic DSC experiments were performed to determine the glass-transition temperatures (T_g's) of the completely cured materials. Samples were heated from room temperature to 250°C at 10°C/min, then cooled in the DSC cell to room temperature, and immediately reheated to 250°C at 10°C/min. The T_g was taken as the midpoint of the endothermic step transition.

XRD of the parent clay, purified clay (MMT), OMMT, and cured composite systems were performed with a Philips PW 1010 X-ray diffractometer (Eindhoven, The Netherlands) with Cu Kα radiation operating at 40 kV and 20 mA. Purified MMT and OMMT were also characterized with simultaneous DSC–TGA on a Netzsch thermoanalyzer STA 409. Samples were heated from room temperature to 1050°C at a heating rate of 10°C/min in a synthetic air flow.

RESULTS AND DISCUSSION

The XRD patterns of purified clay (MMT) before and after alkylammonium treatment indicated the exchange of inorganic cations between the MMT layers with the long-chain alkylammonium ions. The inter-

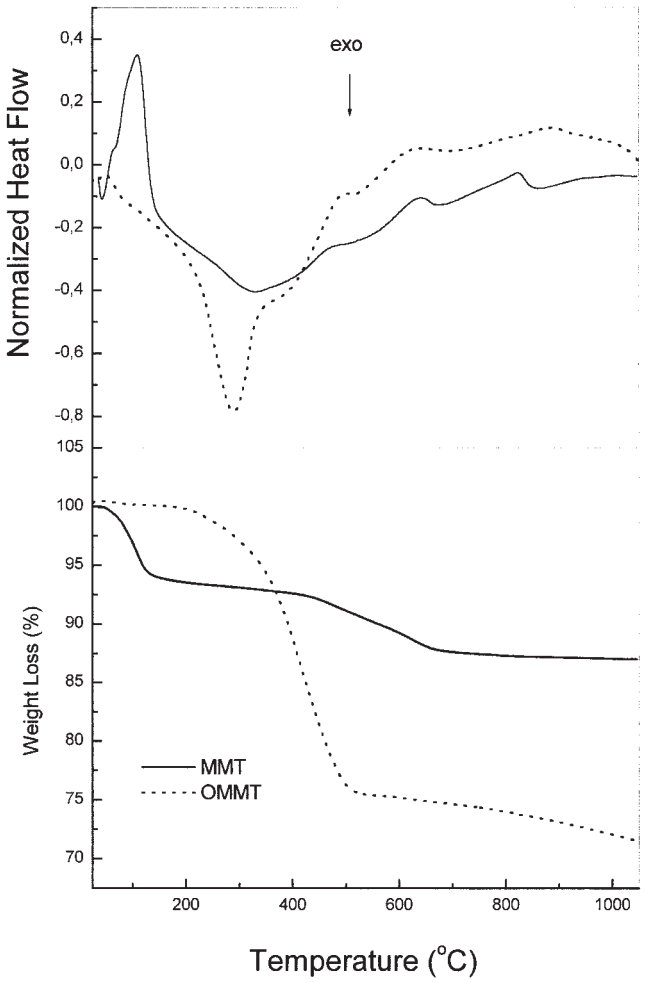

Figure 1 DSC–TGA curves for purified clay (MMT) and OMMT.

lamellar spacing of the clay, corresponding to the (001) plane peak, increased from 13.42×10^{-10} m for MMT to 21.9×10^{-10} m for OMMT. The obtained basal spacing (001) was comparable to the results reported in the literature.[8]

In Figure 1, the results of simultaneous DSC–TGA of MMT and OMMT are shown. The first endothermic peak on DSC curve (bellow 150°C) is assigned to the loss of adsorbed water.[12] In comparison to the unmodified MMT the OMMT is characterized by the endothermic peak of lower intensity and lower mass loss indicating that OMMT is less hydrophilic than MMT. At temperature higher than 200°C the thermal degradation of alkylammonium ions in OMMT begins. This reaction of thermal degradation is well known as Hofmann elimination.[27] From the differences in the loss on ignition of the dried OMMT and corresponding unmodified MMT and the molecular weight of the organic modifier the cation exchange capacity of 103 mequiv/100 g was obtained what is close to the value determined by ammonium acetate method (101 mequiv/100 g).

Figure 2 shows the XRD patterns of OMMT and fully cured investigated composite systems. A peak situated around $2\theta = 20°$ whose intensity increases with OMMT content in composite is observed. This peak corresponds to (110) crystallographic plane of the MMT and confirms the presence of the MMT in the composite. The broad peak between 2θ of 10–25° corresponds to the amorphous epoxy matrix. The absence of basal spacing (001) in both composite systems is observed. It is common practice to classify a nanocomposite as fully exfoliated from the absence of (001) reflections. However, as literature data[8] indicated the large distribution of basal spacing may cause the absence of (001) reflections as well. It should be noted that all cured samples were optically transparent indicating that the size of inorganic phase is smaller than the wavelength of visible light.

Figure 3 shows isothermal DSC curves of the composite system containing 5 phr of OMMT. In isothermal DSC, there is a brief period of temperature stabilization after the sample is introduced into the instrument. Because of that, isothermal DSC curves have to be corrected, extrapolating the value of the heat flow to time = 0. Rescanning of the isothermally cured samples indicated residual reactivity although all investigated isothermal cure temperatures were higher than the T_g's of completely cured materials: 79°, 85° and 86°C for epoxy and nanocomposites with 5 and 10 phr of OMMT, respectively. Figure 4 shows dynamic DSC curves for investigated systems recorded after

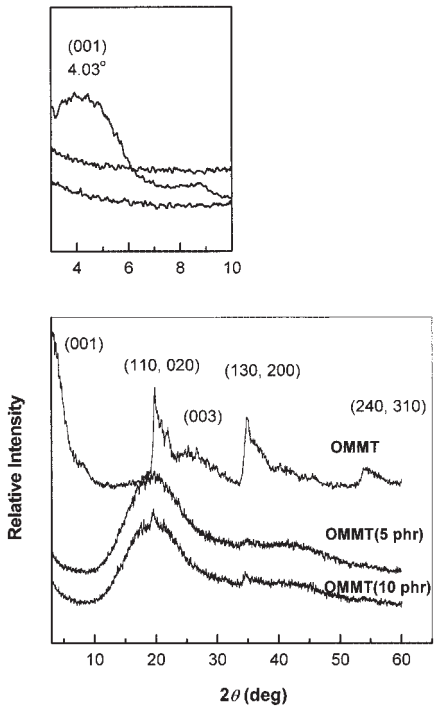

Figure 2 XRD patterns of OMMT and the fully cured composite systems.

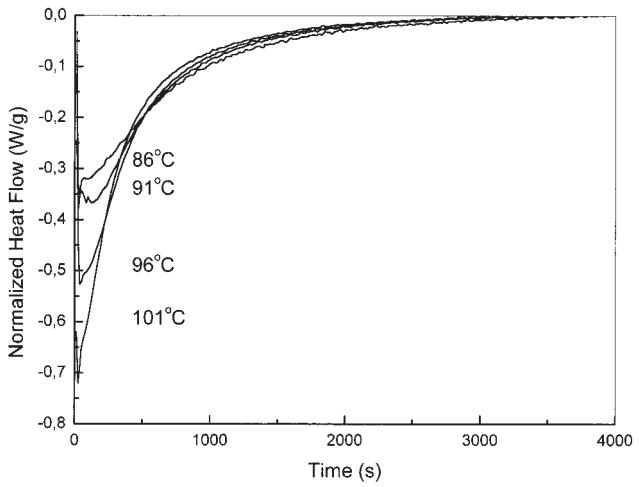

Figure 3 Isothermal DSC curves for the composite system containing 5 phr OMMT at the reported temperatures.

TABLE II
H_I and H_R Values for the Investigated System and T_g Values of the Isothermally Cured Samples

OMMT (phr)	Temperature (°C)	H_I (J/g)	T_g (°C)	H_R (J/g)	$H_I + H_R$ (J/g)	$H_I + H_R$[a] (J/g)
0	91	−303	63.7	−46	−349	
	96	−327	69.3	−20	−347	
	101	−362	72.8	−16	−378	
	106	−354	75.0	−13	−367	
5	86	−278	62.1	−37	−315	
	91	−270	64.6	−26	−296	334
	96	−294	71.3	−11	−305	364
	101	−296	72.6	−9	−306	353
10	86	−272	63.7	−33	−305	
	91	−301	64.7	−10	−311	322
	96	−332	69.0	−6	−338	351
	101	−290	66.1	−7	−298	341

[a] Calculated from the neat resin curing agent data.

isothermal runs at reported temperatures. For comparison DSC scans showing glass transition of completely cured materials are shown as well. As seen, relatively small changes in the T_g were observed for the nanocomposites in comparison to the cured epoxy resin. Similar results are reported in the literature.[15] The T_g values of isothermally cured samples are listed in Table II together with values of the isothermal heat of the reaction (H_I) and the H_R, which obtained according to the procedure described in the Experimental section. For composite system the sum of H_I and H_R determined experimentally is lower than $H_I + H_R$ calculated from the neat epoxy–curing agent data (see the last column in Table II). The possible explanation for this findings is that a part of the reaction heat released is consumed in endothermic exfoliation of nanofiller.[7] Another reason could be the change of the heat capacity of the system due to the addition of the filler.

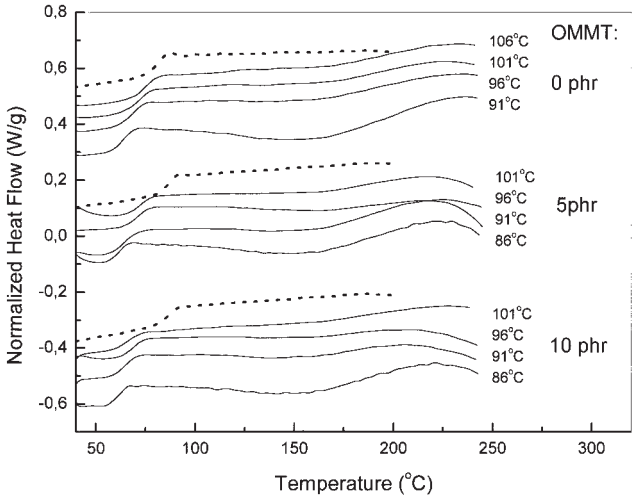

Figure 4 Dynamic DSC curves for the investigated systems recorded after isothermal runs at the reported temperatures. For comparison, the dynamic DSC curves of completely cured samples are also given (dotted lines).

To relate the heat evolution in the DSC experiment to the epoxide conversion, it is necessary to assume that the heat released on reaction of an epoxide group is the same regardless of the type of epoxy or the nature of the reaction. The results reported in the literature[22] support this assumption. The reaction rate ($d\alpha/dt$) as a function of time (t) was calculated from the rate of heat flow (dH/dt) as measured in the DSC experiments by the following equation:

$$\frac{d\alpha}{dt} = \frac{1}{H_T}\frac{dH}{dt} \tag{1}$$

The total heat developed during DSC tests ($H_T = H_I + H_R$) was taken as the basis for the ultimate fractional conversion. By partial integration of the areas under the isothermal $d\alpha/dt$ curves, the fractional conversion (α) as a function of time was obtained:

$$\alpha = \frac{1}{H_T}\int_0^t \frac{dH}{dt}dt \tag{2}$$

The $d\alpha/dt$ and the α as functions of time at 96°C for investigated systems are illustrated in Figure 5. The maximum in the $d\alpha/dt$ versus time curve at time 0 (after the start of the reaction) is a characteristic of autocatalytic reactions. As the amount of OMMT increased the maximal $d\alpha/dt$ increased as well what can be explained as the catalytic effect of intercalated acidic octadecylamine ions in OMMT on the epoxy polymerization reactions. The results in Figure 5 also

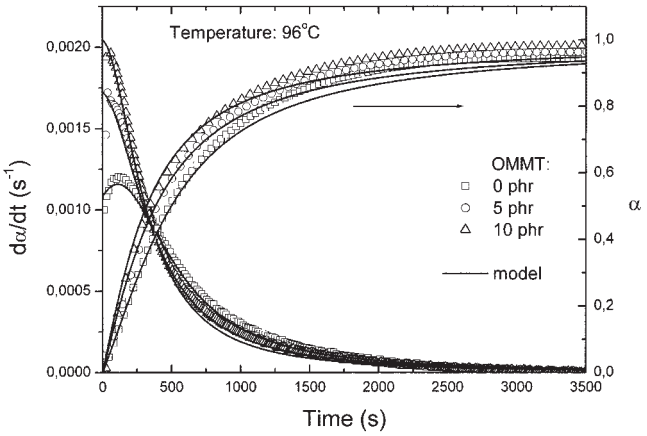

Figure 5 Isothermal $d\alpha/dt$ and α as functions of time for the investigated systems at the reported temperature and a comparison of the experimental data with the kinetic model data.

show that the presence of OMMT in epoxy resin does not change the autocatalytic nature of reaction. Similar findings are reported in the literature.[17] The $d\alpha/dt$ profiles of investigated systems obtained in dynamic (constant heating rate) conditions are compared in Figure 6. In comparison to neat resin/curing agent system a shift of composite curves to lower temperatures is seen what may also indicate the catalytic effect of octadecylamine ions on the epoxy polymerization reactions. To illustrate this effect the temperatures of the maximal $d\alpha/dt$ at different heating rates are compared in Table III.

The essential step in the study of cure kinetics by DSC is fitting of the $d\alpha/dt$ profiles to a kinetic model. Because of the complex nature of thermosetting reactions, phenomenological models are the most popular for these systems. However, they do not provide any

TABLE III
Temperatures of Exothermal Peaks $T_{max's}$ Obtained from Nonisothermal Measurements at Different Heating Rates

Heating rate (°C/min)	T_{max} (°C)[a]		
	0	5	10
3	102.3	96.2	91.4
5	112.7	106.0	102.3
10	127.5	121.2	114.3

[a] The numbers shown below the line are grams of OMMT per 100 g of epoxy.

information about the reaction path that is important for understanding the network formation process. In this work the following model[28] arising from the kinetic mechanism proposed by Horie et al.[29] was applied to our data, and model predictions were compared to experimental results:

$$\frac{d\alpha}{dt} = k(\alpha + B)(1 - \alpha)(r - \alpha) \tag{3}$$

where k is the reaction rate constant, the product kB is the initial reaction rate, and r is the initial ratio of amine N—H bonds to epoxide rings, respectively. In the derivation of eq. (1) equal reactivity of all amino hydrogens (primary and secondary) has been assumed.

It is generally agreed, that in the reaction between epoxides and amines, the addition occurring in two stages is the most important:

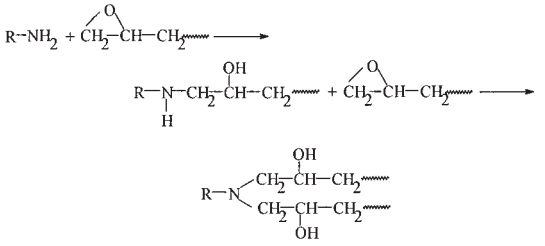

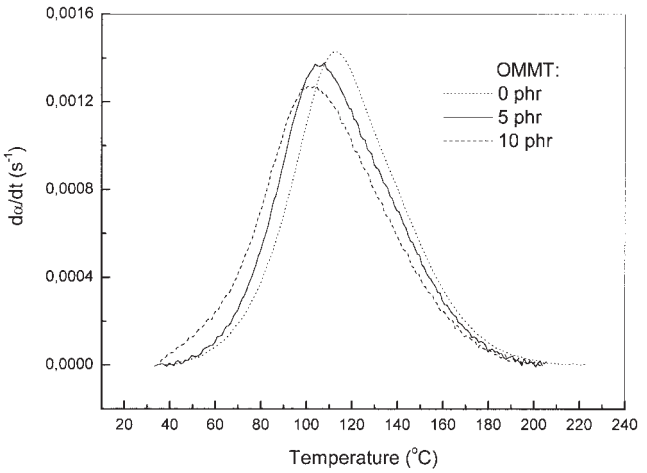

Figure 6 $d\alpha/dt$ as a function of temperature for the investigated systems at a heating rate of 5°C/min.

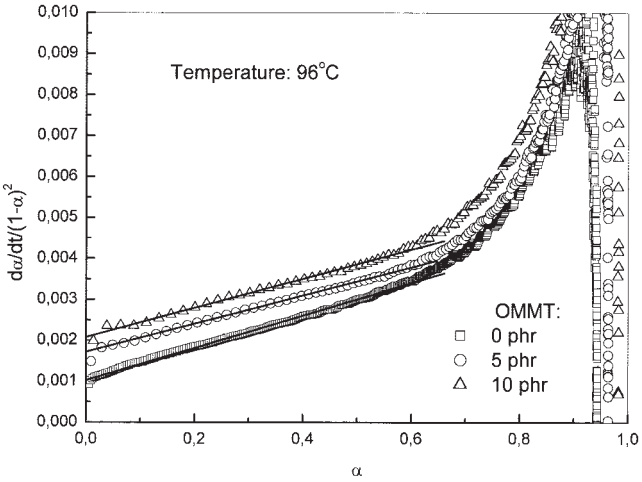

Figure 7 Plot of $(d\alpha/dt)/(1 - \alpha)^2$ as a function of α for the investigated systems at the reported temperature.

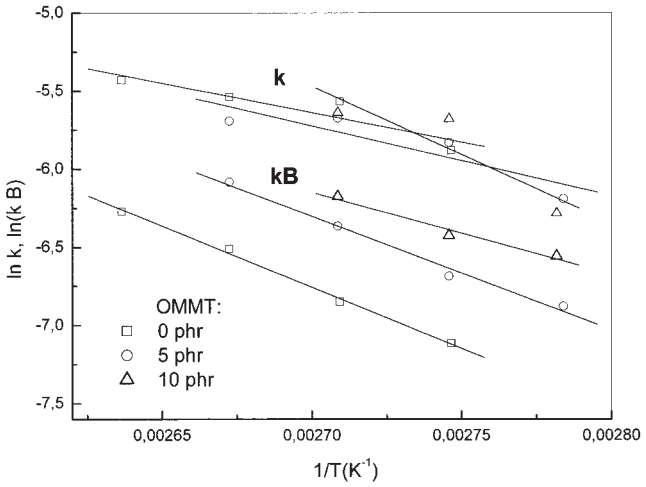

Figure 8 Arrhenius plots of the isothermal k and kB values determined from the data analysis according to autocatalyzed reaction kinetics.

(4)

To describe the kinetics of the epoxy reaction with amines, Horie et al.[29] took into account the autocatalytic action of the hydroxyl groups formed during the reaction and assumed that some catalyst or impurity is initially present in the system.

From the rearranged eq. (3)

$$\frac{d\alpha/dt}{(1-\alpha)(r-\alpha)} = k\alpha + kB \tag{5}$$

the parameters k and B can be determined by plotting $(d\alpha/dt)/[(1-\alpha)(r-\alpha)]$ versus α.

For a stoichiometric mixture in which the number of epoxide rings is just sufficient to react with all the N—H bonds present $r = 1$. As illustrated in Figure 7, a good correlation of $(d\alpha/dt)/(1-\alpha)^2$ versus α data was obtained up to approximately 60% conversion for all investigated system. The deviation of $(d\alpha/dt)/(1-\alpha)^2$ versus α data from the straight line at higher conversion can be attributed to the occurrence of an another reaction (e.g., the etherification reaction)[22]

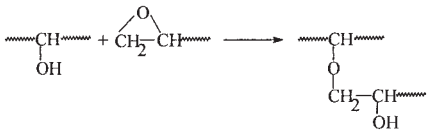

(6)

in addition to the epoxy–amine reaction.

We have recently showed[30] for similar epoxy system that complete epoxy cure can be fairly described by dividing the $d\alpha/dt$ profiles in the contributions from two assumed reactions (epoxy–amine and etherification reactions).

k and kB (reported in Table IV) depend on the temperature following the Arrhenius relationship (as shown in Figure 8):

$$k = A\exp(-E_a/RT) \tag{7}$$

where A is a preexponential factor, E_a is the activation energy, R is the gas constant, and T is the absolute temperature. A plot of ln kB versus $1/T$ was used to determine the activation energy for the reaction catalyzed by groups initially present in the resin (E_{a1}). From the linear least-squares fit of ln k versus $1/T$ data, the activation energy for the epoxy–amine reaction catalyzed by newly formed hydroxyl groups (E_{a2}) was determined. The Arrhenius parameters (preexponential factors A_1 and A_2 and E_{a1} and E_{a2} values) are given in Table IV as well. With the increase of OMMT amount in the system a decrease in E_{a1} and an increase in E_{a2} is obtained.

To see the extent of error if only epoxy–amine reactions are taken into account eq. (3) was solved numerically by the Runge–Kutta method for each investigated temperature. Comparisons between the experimental data and the model predictions are given in

TABLE IV
Parameters of the Autocatalytic Kinetic Model [Eqs. (3) and (7)] for the Investigated Systems

OMMT (phr)	Temperature (°C)	$10^3\ kB$ (s^{-1})	$10^3\ k$ (s^{-1})	ln A_1	E_{a1} (kJ/mol)	ln A_2	E_{a2} (kJ/mol)
0	91	0.81	2.79	14.39	65.1	4.54	31.3
	96	1.06	3.82				
	101	1.49	3.93				
	106	1.89	4.38				
5	86	1.03	2.05	13.3	60.4	6.3	37.1
	91	1.25	2.94				
	96	1.72	3.44				
	101	2.28	3.37				
10	86	1.42	1.87	8.0	43.5	18.2	72.9
	91	1.62	3.42				
	96	2.08	3.56				
	101						

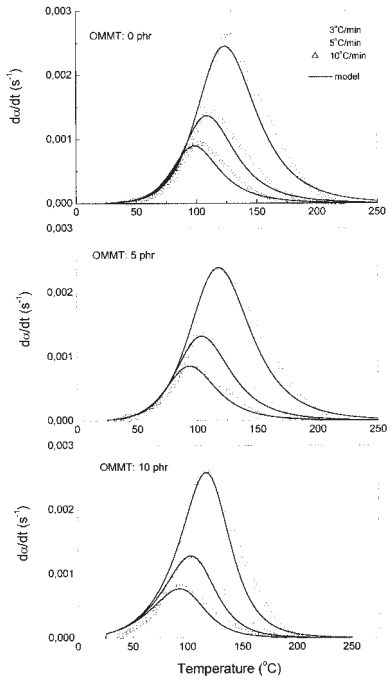

Figure 9 Comparison of experimental data with the kinetic model data: $d\alpha/dt$ as a function of temperature for the investigated systems at the reported heating rates.

Figure 5 as well. As expected the extent of reaction at the later stage of cure is slightly underestimated but for practical purposes model predictions are fairly good.

One of the drawbacks of isothermal curing is the limited temperature range where useful kinetic information may be obtained. The modeling of the industrial processing requires a knowledge of the curing kinetics in a broad temperature range. To see if the kinetic expressions arising from isothermal runs are valid outside the range of temperature used for parameter fitting the cure in dynamic conditions, at constant heating rates, was simulated as well. Comparisons between the experimental data obtained in dynamic DSC runs at different heating rates and the model predictions are presented in Figure 9. The model predicts fairly well the beginning of cure, the maximal $d\alpha/dt$ and the end of reaction what is important for practical purposes (to estimate appropriate processing conditions for materials). To predict the shoulder in $d\alpha/dt$ profile observed at higher temperatures etherification reaction should be taken into account.

CONCLUSIONS

The isothermal and nonisothermal reaction kinetics of an epoxy/poly(oxypropylene)diamine/OMMT system were studied by means of DSC. Results indicated that the intercalated onium ions catalyze epoxy–amine polymerization. A kinetic model, arising from an autocatalyzed reaction mechanism was applied to isothermal DSC data. The presence of OMMT in epoxy resin does not change the autocatalytic nature of reaction. In the investigated systems E_{a1} decreased whereas E_{a2} increased with the addition of OMMT. The kinetic model with parameters determined from isothermal DSC data satisfactorily describes the cure in the dynamic (constant heating rate) conditions.

References

1. Wang, M. S.; Pinnavaia, T. J. Chem Mater 1994, 6, 468.
2. Messersmith, P. B.; Giannelis, E. P. Chem Mater 1994, 6, 1719.
3. Lan, T.; Pinnavaia, T. J. Chem Mater 1994, 6, 2216.
4. Lan, T.; Kaviratna, P. D.; Pinnavaia, T. J. Chem Mater 1995, 7, 2144.
5. Lan, T.; Kaviratna, P. D.; Pinnavaia, T. J. J Phys Chem Solids 1996, 57, 1005.
6. Brown, J. M.; Curliss, D.; Vaia, R. A. Chem Mater 2000, 12, 3376.
7. Jiankun, L.; Yucai, K.; Zongneng, Q.; Xiao-Su, Y. J Polym Sci Part B: Polym Phys 2001, 39, 115.
8. Kornmann, X.; Lindberg, H.; Berglund, L. A. Polymer 2001, 42, 1303.
9. Kornmann, X.; Lindberg, H.; Berglund, L. A. Polymer 2001, 42, 4493.
10. Chin, I. J.; Thurn-Albrecht, T.; Kim, H. C.; Russell, T. P.; Wang, J. Polymer 2001, 42, 5947.
11. Butzloff, P.; D'Souza, N. A.; Golden, T. D.; Garrett, D. Polym Eng Sci 2001, 41, 1794.
12. Chen, K. H.; Yang, S. M. J Appl Polym Sci 2002, 86, 414.
13. Park, S. J.; Seo, D. I.; Lee, J. R. J Colloid Interface Sci 2002, 251, 160.
14. Suh, D. J.; Park, O. O. J Appl Polym Sci 2002, 83, 2143.
15. Triantafillidis, C. S.; LeBaron, P. C.; Pinnavaia, T. J. J. Solid State Chem 2002, 167, 354.
16. Salahuddin, N.; Moet, A.; Hiltner, A.; Baer, E. Eur Polym J 2002, 38, 1477.
17. Xu, W. B.; Bao, S. P.; Shen, S. J.; Hang, G. P.; He, P. S. J Appl Polym Sci 2003, 88, 2932.
18. Morgan, R. J.; Mones, E. T. J Appl Polym Sci 1987, 33, 999.
19. Musto, P.; Martuscelli, E.; Ragosta, G.; Russo, P.; Villano, P. J Appl Polym Sci 1999, 74, 532.
20. Mijovic, J.; Andjelic, S. Macromolecules 1995, 28, 2787.
21. Barton, J. M. Adv Polym Sci 1985, 72, 112.
22. Cole, K. C.; Hechler, J. J.; Noel, D. Macromolecules 1991, 24, 3098.
23. Opalicki, M.; Kenny, J. M.; Nicolais, L. J Appl Polym Sci 1996, 61, 1025.
24. Boey, F. J. C.; Qiang, W. Polymer 2000, 41, 2081.
25. Mauri, A. N.; Riccardi, C. C. J Appl Polym Sci 2002, 85, 2342.
26. Firouzmanesh, M. R.; Azar, A. A. Polym Int 2003, 52, 932.
27. Solomons, T. W. G. Organic Chemistry; Wiley: New York, 1996.
28. Wisanrakkit, G.; Gillham, J. K. J Appl Polym Sci 1990, 41, 2885.
29. Horie, K.; Hiura, H.; Sawada, M.; Mita, I.; Kambe, H. J Polym Sci Part A-1: Polym Chem 1970, 8, 1357.
30. Macan, J.; Brnardic, I.; Ivankovic, M.; Mencer, H. J. J Therm Anal Cal 2005, 81, 369.